Effects of Bosch Scallops on Metal Layer Stress of an Open Through Silicon Via Technology

A.P. Singulani[a,b], *H. Ceric*[a,b], *and E. Langer*[a]
[a]Institute for Microelectronics, TU Wien
[b]Christian Doppler Laboratory for Reliability Issues in Microelectronics
at Institute for Microelectronics Vienna, Austria
{singulani|ceric|langer@iue.tuwien.ac.at}

S. Carniello
AMS A. G.
Unterpremstätten, Austria
sara.carniello@ams.com

***Abstract*—Through Silicon Via (TSV) is a lead topic in interconnects and 3D integration research, mainly due to numerous anticipated advantages. However, several challenges must still be overcome if large scale production is to be achieved. In this work, we have studied effects of Bosch scallops concerning mechanical reliability for a specific TSV technology. The presence of scallops on the TSV wall modifies the stress distribution along the via. By means of Finite Element Method (FEM) simulations, we could assess this change and understand the process. The achieved results support experiments and give a better insight into the influence of scallops on the stress in an open TSV.**

Through Silicon Via; TSV; Simulation; Reliability

I. INTRODUCTION

Thermal and intrinsic stresses are responsible for several reliability issues related to TSVs. Consequently, they have become a major concern in mechanical stability design [1-3]. The thermo-mechanical stress arises from the difference between the coefficient of thermal expansion (CTE) of the silicon and the interconnection metal. At the same time the intrinsic stress results from different physical mechanisms that take place during metal deposition.

The impact of each stress can be controlled by the choice of the materials and the geometry which form the TSV. A good design should manage the mechanical issues while it ensures the electrical functionality of the device. One of the most common and well documented layouts is the cylindrical copper TSV. The good electrical properties of copper and the fabrication easiness are clear advantages of this technology. However, the difference of more than one order of magnitude between silicon and copper CTEs negatively affects the mechanical reliability.

CTE mismatch can be compensated by different strategies, for instance by usage of polymer liners around the TSV [4]. The liners work as a barrier that absorbs the stress and hinder its spread towards the silicon. Another approach is the use of an open (unfilled) TSV instead of a filled via [4][5]. This scheme reduces the amount of material in the structure and provides room for the metal to expand freely towards the axis of the via leading to an overall stress reduction. Additionally, the stress induced by the TSVs in the silicon can be attenuated by a particular placement of them [5]. A device has usually several vias close to each other, which can be arranged in a such way so that stress is mutually cancelled or reduced among them.

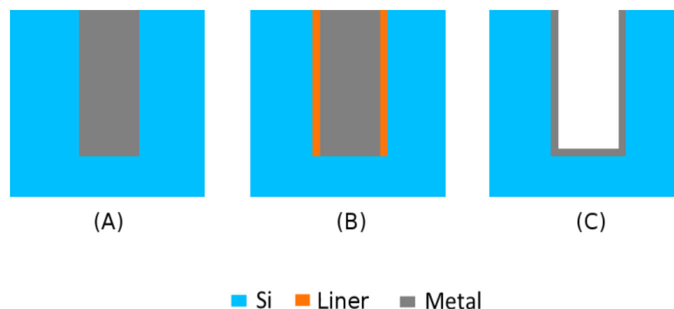

Figure 1. Three cylindrical TSV designs: Filled (A), filled with liners (B), and open (C).

It was recently introduced a 3D integration technology based on open TSV [5], and since then several papers have been published about its mechanical [5-7] and electrical properties [8]. So far, the structure has proved itself to be reliable and mechanical stable, but a recent paper of Krauss [6] reported an uncommon behavior of the stress in the via. Krauss *et al.* performed mechanical characterization of the structure and learned that the intrinsic stress inside TSV's metal layers was four times smaller than expected. This phenomenon was not entirely understood, although Krauss *et al.* has identified Bosch scallops – that are created during open TSVs processing – as a possible cause. The description of such a phenomenon is important since it affects capability to predict failure scenarios.

In this work, we investigated the stress distribution by mechanical simulations of the structure. Our goal was to provide an explanation for the stress reduction and assess the impact of Bosch scallops on mechanical reliability of an open TSV technology.

II. PROBLEM DESCRIPTION

A. Structure

The presented integration technology uses wafer bonding and TSVs in order to integrate low output sensors with their associated analog amplification and signal processing circuitry (Fig. 2). Metallization and SiO_2 passivation are deposited conformally on the TSV surfaces following the Si etch process. More processing details can be found in the work of J. Kraft *et al.* [8]. The metal layers were composed of tungsten (W) and Ti/TiN thin films with thickness of 100 nm and 95 nm, respectively (Fig. 2).

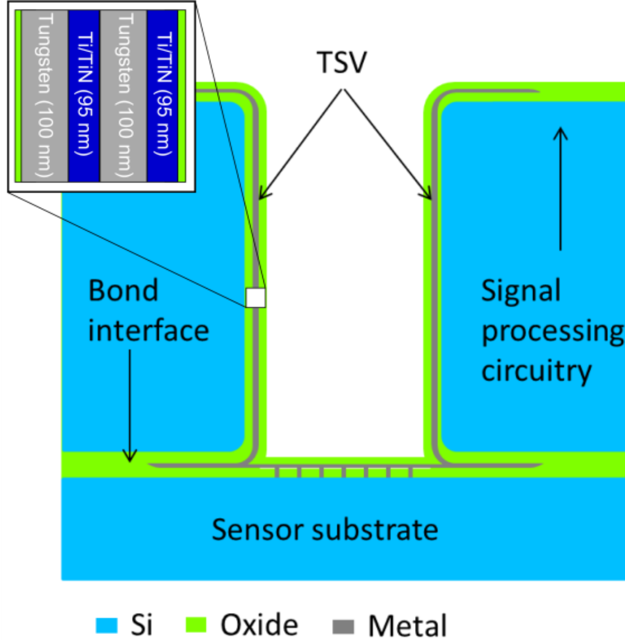

Figure 2. Schematic cross section of the open TSV technology used in this work. Metal layers composition and thickness are depicted on detail.

B. Stress divergence

C. Krauss *et al.* performed X-Ray Diffraction (XRD) stress measurements on the metal layers of this structure [6], but a specific TSV geometry has permitted the measurements only to the top 10 µm. A full plate sample with an identical layer profile is then used to support stress characterization (Fig. 3). The purpose of the full plate is to ease the measurement process and to improve its precision. Additionally, It represents the best estimation for the stress on the middle of the via since it is unfeasible to measure it deeper on the TSV. However, the stress on the TSV tungsten film was found to be smaller than in the full plate samples. At the TSV's wall, scallops were observed which were caused by the Bosch process (Fig. 5) itself. The presence of scallops suggests that they might be the reason behind the stress reduction.

To explain the stress differences between the samples, we studied the effects of the scallops on vias by Finite Element Analysis (FEA). We hypothesized that the scallop's geometry causes the stress reduction. Furthermore, a possible weak adhesion of the scallops bottom due to shadowing effects was also investigated. This phenomenon can lead to stress relaxation and can also explain the difference between the measurements.

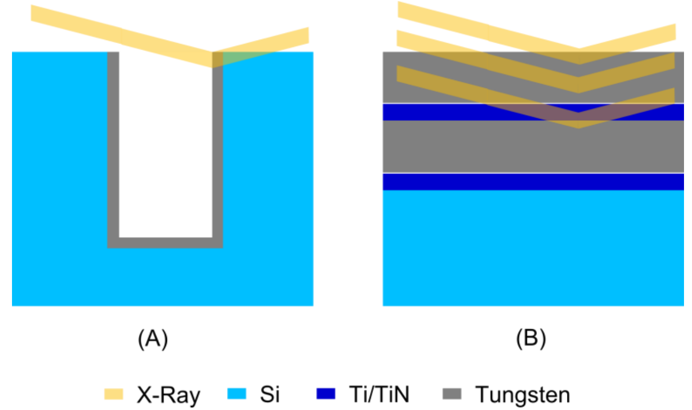

Figure 3. X-Ray measurement for TSV sample (A) and full plate sample (B). The geometry of the TSV prevents good penetration of the x-rays on the tungsten layer, therefore full plate samples are needed for better analysis.

III. SIMULATION SETUP

To evaluate our hypotheses, mechanical simulations were performed on two structures (Fig. 4). An initial tensile intrinsic stress of 1600 MPa was assumed on the tungsten layers, as measured on the full Plate samples [6]. The material interfaces of the scallops' bottom were treated as a contact surface, thus the weak adhesion was approached properly. The solution of the resulted surface problem is computed by a combination of Lagrange and penalty method as described by Faraji [9]. More details about the contact mechanics is out of this paper scope but further implementation and modeling details can be obtained elsewhere [9][10].

The numerous small contact surfaces have made the simulation a challenging task. As a first approximation a simple structure was used to reduce the numerical difficulties (Fig. 4a). This structure lacks some layers in comparison to the original TSV. The experience acquired through the simulation of this simple structure regarding assumptions, numerical issues, meshing and physical interpretation is then carried over to a more complex arrangement (Fig. 4b). This elaborated structure contains the entire set of layers of the TSV in question. This structure was used for the final analysis and comparison with experimental data.

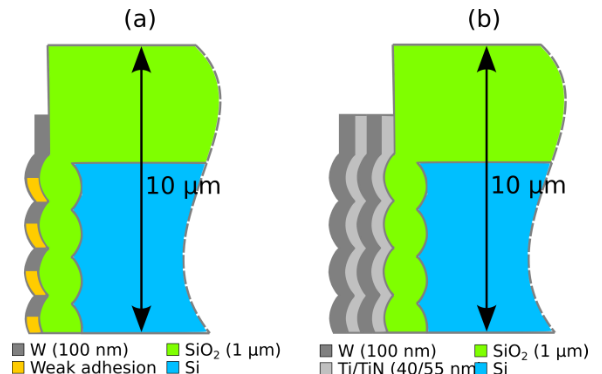

Figure 4. (a) Simple structure used for weak adhesion study: only a single layer is considered. (b) Complex and realistic structure with all layers present.

A. *Scallop geometry*

An accurate evaluation of our hypothesis relies on a good description of the scallop's form. They presented a parabolic-like shape as depicted on the cross section TSV's images (Fig. 5). The height and width is estimated to 2 µm and 0.5 µm respectively. The scallop's shape is mimicked in our simulation by rational quadratics Bézier curves [11] which the general form is given by

$$B(t) = \frac{(1-t)^2 P_0 W_0 + 2t(1-t) P_1 W_1 + t^2 P_2 W_2}{(1-t)^2 W_0 + 2t(1-t) W_1 + t^2 W_2}. \quad (1)$$

Where P_0, P_1, and P_2 are control points as depicted in Fig. 6. W_0, W_1, and W_2 are weights used for curvature control and t is the curve parameter that varies between 0 and 1.

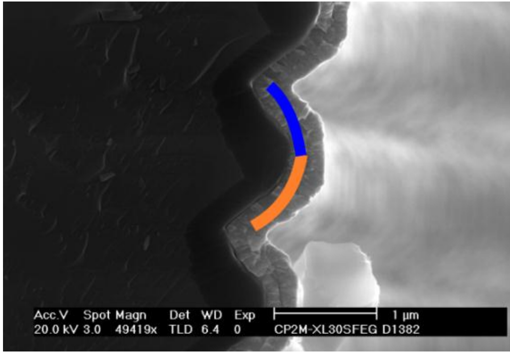

Figure 5. Cross section of the TSV wall with the scallops. Our best Bézier curve approximation (W=1/3) is also displayed.

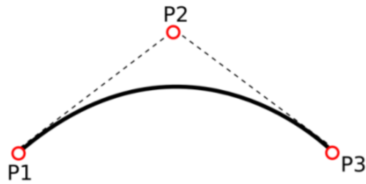

Figure 6. General form of a quadratic Bézier curve.

Two Bézier curves were used to form a scallop (Fig. 7). For each scallop, the curvature, size and width were controlled by a suited chose of weights and points relation of both curves, following the rules below

- P1 and P6 must be on the intended TSV wall (without scallops) and the distance between them defines scallop's width.
- The distance between P1 and P2 defines the maximum scallop's height which is reached at the middle of the scallop's width.
- P1 and P2 are placed on the same side of the scallop and P5 and P6 are placed on the opposite side of the scallop.
- The weights W_1, W_3, W_4, and W_6 have the value 1. The weights W_2 and W_5 have the same value (which controls the scallop's curvature), W_2=W_5=W. We have chosen W=1/3.

Although our approach describes scallops parabolic shape, the junction between them is smoother than the Bézier curve can represent. This could lead to singularities during simulation, resulting in high stress on those points.

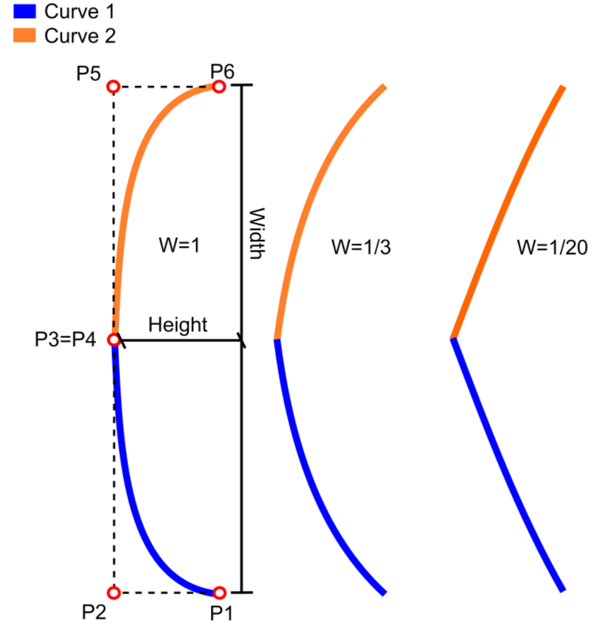

Figure 7. Representation of scallops by Bézier curves. W controls the shape of the curve and each curve is defined by three points.

B. *Meshing and Boundary conditions*

The simulation of the entire structure (as depicted in Fig. 2) is computational unfeasible in the presence of a great number of scallops and contact surfaces. Thus, we reduced the simulation domain (Fig. 8) taking into consideration the aforementioned experimental constraint (10 µm from the top of the TSV).

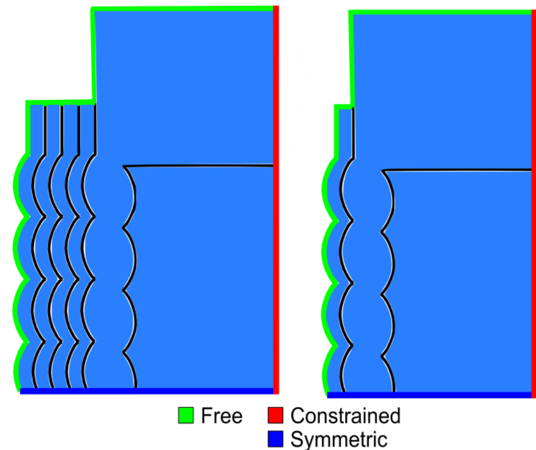

Figure 8. Simulation domain for both structures (complex and simple, respectively). The boundaries conditions are also indicated.

As boundary conditions we assumed the extreme right side of the structure fixed, while the TSV's inner side is free to move as well as the top (Fig. 8). The bottom boundary has a more complicated scenario, because a proper condition is unknown in the adopted domain. To handle this situation we used symmetric boundary condition (Fig. 8). Although this is not true when the whole structure is considered, it is a good approximation for the geometry around the simulation domain. Additionally, it reduces any possible boundary effect that could impact the solution. The simulation was performed over axisymmetric assumption to capture the cylindrical shape of the TSV.

The scallops shape and the contact surfaces demand a fine mesh to prevent numerical procedure convergence issues (Fig. 9). As a result the mesh is rather complex near the scallops, leading to big meshes for a relatively small structure. Triangular elements were used because they showed a better adaptability in this structure in comparison to quadrilateral elements. The mesh of the structure A has 17945 points and 35461 triangles and the structure B 12466 points and 24635 triangles.

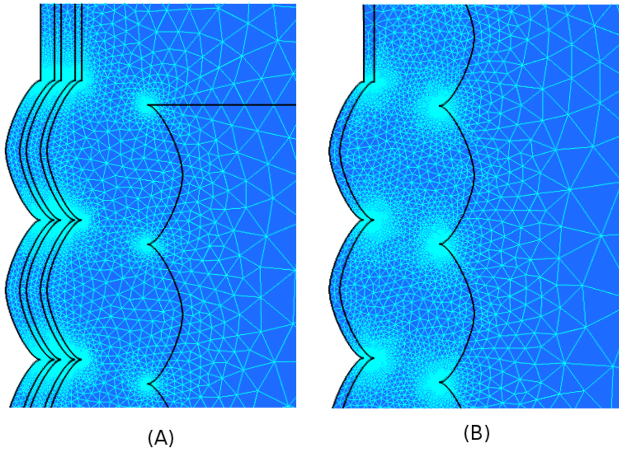

Figure 9. Meshes for the complex structure (A) and the simple structure (B) with the scallops in detail.

IV. Results

We have simulated three cases using the following structures: TSV without scallops, TSV with scallops, and TSV with weak adhesion. The first case was performed to control the hypothesis, whereas the other two cases were used for an evaluation of each particular feature on stress. The geometry of the scallops has been identified as the main cause for stress reduction inside the tungsten layer (Fig. 10). Although the weak adhesion has induced some relaxation (~ 17%), it superimposes to a stress state already reduced by the geometry. Moreover, the in-plane stress on tungsten is not equal in every direction in the presence of scallops. Krauss *et al.* was unaware of this fact and assumed an in-plane equibiaxial condition for the stress [6]. Consequently, the reported stress does not characterize the state in the tungsten layer, but rather the average normal stress in z-direction, according to the described experimental setup.

The complex structure was simulated under the same conditions as the simple one, except in the weak adhesion case, which was not considered (Fig. 11). Since the equibiaxial stress assumption is not valid in the case of the scallops' presence, the simulated and experimental stress results have not been compared. Instead, the strain was compared, which is a direct measure and free of any premise.

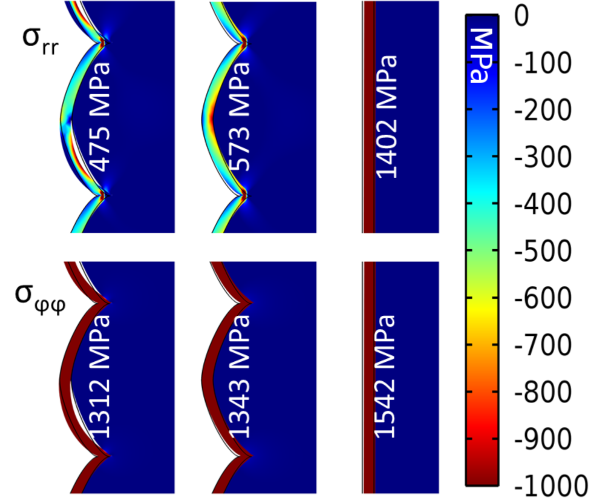

Figure 10. Average normal stress on simple structure (written in white) for each situation: weak adhered, no-weak adhered, and flat scallops respectively.

The average simulated strain of 0.00169 in the z-direction was in reasonable agreement with the measured strain of 0.00111 [6] for the tungsten layer. We disconsidered the intrinsic stress on Ti/TiN layers due to the unavailability of experimental data by the time of this publication. But simulations considering a compressive stress of 1.0 GPa in Ti/TiN layers resulted on an average strain of 0.00127 in tungsten. Hence, the absence of the intrinsic stress on Ti/TiN can justify the difference between simulated and experimental data. This comparison has validated the simulation setup and underlines its applicability for further analysis.

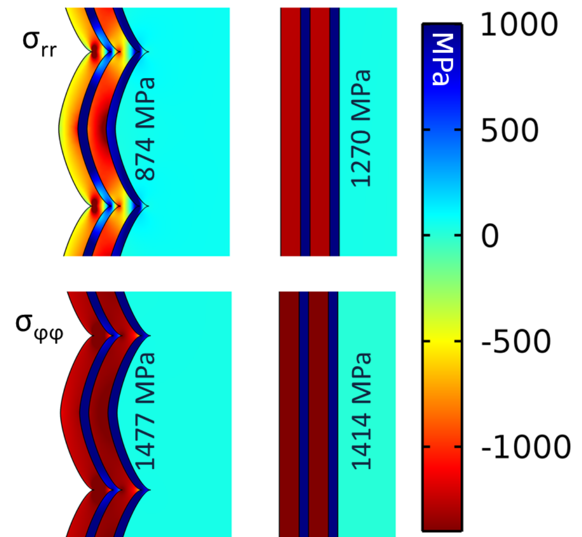

Figure 11. Average normal stress on the real structure (written in black).

The rigidity (small-scale variation) characteristic of the scallops in the z-direction modifies stress distribution in TSV films. The tensile stress induces an inward movement in the region of valleys between scallops (Fig. 12). This leads to a relief of the stress along the via since the material finds a favorable point to stretch. Consequently, the average normal stress in the z-direction in tungsten is reduced, causing the difference between TSV and full plate samples. However, in the phi-direction there is no stress reduction. Along this axis the geometry is not modified by the scallops. Therefore the initial load faces the same scenario in the presence or absence of scallops.

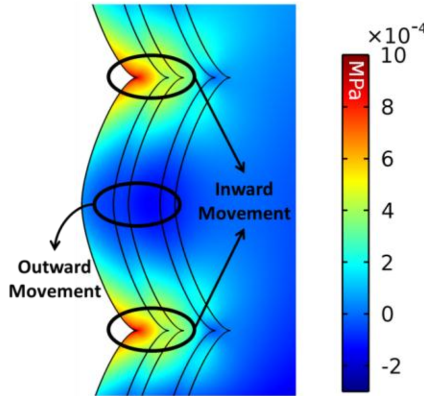

Figure 12. Displacement in R-direction.

Additional insight concerning reliability is gathered from an analysis of the Von Mises stress. The mean values for structures with and without scallops were 1268 MPa and 1360 MPa respectively. Since there is not a significant difference, the full plate sample measurements could be used safely for average Von Mises stress. However, the mean value did not suffice when the scallops were present due to the changing stress distribution. Fig. 13 outlines the accumulation stress points. The Von Mises stress can reach 6500 MPa, which is considerably higher than the 1500 MPa, experienced on full plate samples. However, such high value could be the result of the sharp transition between the Bézier curves used to represent the scallops (Singularity points). In spite of that, those points are a region of potential failure, as increased stress could lead to a fracture in the metal.

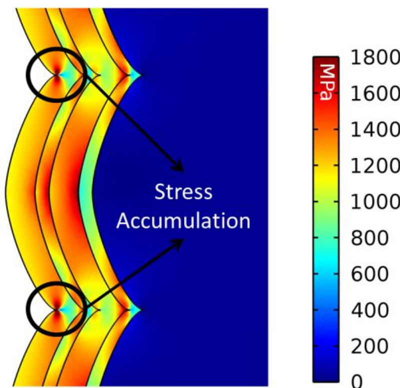

Figure 13. Von Mises stress on real structure. Critical points are indicated. The scale is saturated for better visualization. Max stress value is 6500 MPa.

V. Conclusion

Effects of Bosch scallops on stress reduction in metal layers of an open TSV technology were studied. Two possibilities were evaluated for an explanation for the phenomenon, those being weak adhesion of the scallops' bottom and the geometry of the scallops themselves. The latter causes most of the stress reduction, while weak adhesion is only a secondary mechanism. We described the manner in which the scallop's geometry modifies the stress. Additionally, valleys between scallops were identified as potential failure regions. It was also shown that the equibiaxial stress assumption in the vias wall in the presence of scallops is invalid. This information is vital for the proper evaluation of the simulation and experimental results. Finally, the simulation was shown to be consistent with experimental data, validating its setup for further studies.

Acknowledgment

We would like to thanks Christopher Krauss and his colleagues on IM2NP for the measurement data and fruitful discussions. This work was partly supported by the European Union project COCOA.

References

[1] M. Koyanagi, "3D integration technology and reliability", *Proc. IEEE Intl. Reliab. Phys. Symp.*, Monterey, CA, USA, pp. 3F.1.1 – 3F.1.7., 2011.

[2] J. Takahashi, "Through silicon via and 3D wafer/chip stacking technology", *Symp. VLSI Circuits Dig. Tech. Papers*, Honolu, HI, USA pp. 89-92, 2007.

[3] T. V. Baughn, Z. J. Yao, and C. L. Goldsmith, "A new in situ residual stress measurement method for a MEMS thin fixed-fixed beam structure", *Journal of Microelectromech. Syst.*, vol. 11, pp. 309-316, 2002.

[4] K. H. Lu, X. Zhang, S. Ryu, J. Im, R. Huang, and P. S. Ho, "Thermo-Mechanical Relibility of 3-D ICs containing Through Silicon Vias", *Electr. Compon. And Techn. Conf.*, San Diego, CA, USA, pp. 630-634, 2009.

[5] F. Kraft, F. Schrank, J. Teva, J. Siegert, G. Koppitsch, C. Cassidy et al, "3D Sensor application with open through silicon via technology", *IEEE Electr. Comp. and Tech. Conf.*, Lake Buena Vista, FL, USA, pp. 560-566, 2011.

[6] A. P. Singulani, H. Ceric, S. Selberherr, "Thermo-mechanical simulation of an open tungsten TSV", *Proc. IEEE Electr. Packag. Techn. Conf.*, Singapore, pp. 110-114, 2012.

[7] C. Krauss, S. Labat, S. Escoubas, O. Thomas, S. Carniello, J. Teva, F. Schrank, "Stress measurements in tungsten coated through silicon vias for 3D integration", *Thin Solid Films*, in press.

[8] C. Cassidy, J. Kraft, S. Carniello, F. Roger, H. Ceric, A. P. Singulani, E. Langer, F. Schrank, "Through Silicon Via Reliability", *IEEE Trans. Dev. And Mat. Reliab.*, vol. 12, pp. 285-295, 2012.

[9] A. Faraji, Elastic and Elastoplastic Contact Analysis: Using Boundary Elements and Mathematical Programming, vol. 45, WIT Press, 2005.

[10] P. Wriggers, Computational Contact Mechanics, 2nd ed., Springer-Verlag, 2006.

[11] D. Marsh, Appled Geometry for Computer Graphics and CAD, 2nd ed, Springer, pp. 175-185 2005.